Bull. Mater. Sci., Vol. 39, No. 2, April 2016, pp. 405–413. © Indian Academy of Sciences.

Chitosan-encapsulated ZnS : M (M: Fe^{3+} or Mn^{2+}) quantum dots for fluorescent labelling of sulphate-reducing bacteria

H S RAGHURAM[1], SHRAVAN PRADEEP[1], SUBHRA DASH[2], RAJDEEP CHOWDHURY[2] and SONAL MAZUMDER[1,*]

[1]Department of Chemical Engineering, BITS-Pilani, Pilani, Rajasthan 333031, India
[2]Department of Biological Sciences, BITS-Pilani, Pilani, Rajasthan 333031, India

MS received 25 September 2015; accepted 29 October 2015

Abstract. **Chitosan-encapsulated Mn^{2+} and Fe^{3+}-doped ZnS colloidal quantum dots (QDs) were synthesized using chemical precipitation method. Though there are many reports on bio-imaging applications of ZnS QDs, the present study focussed on the new type of microbial-induced corrosive bacteria known as sulphate-reducing bacteria, *Thiobacillus novellus*. Sulphate-reducing bacteria can obtain energy by oxidizing organic compounds while reducing sulphates to hydrogen sulphide. This can create a problem in engineering industries. When metals are exposed to sulphate containing water, water and metal interacts and creates a layer of molecular hydrogen on the metal surface. Sulphate-reducing bacteria then oxidize the hydrogen while creating hydrogen sulphide, which contributes to corrosion for instance, in pipelines of oil and gas industries. In this study, detection and labelling of sulphate-reducing bacteria is demonstrated using fluorescent QDs. Chitosan capped ZnS QDs were synthesized using dopants at different doping concentrations. UV–Vis spectroscopy, XRD and FTIR characterizations were done to identify the optical band gap energy, crystal planes and determine the presence of capping agent, respectively. The morphology and the average particle size of 3.5 ± 0.2 nm were analysed using TEM which substantiated UV–Vis and XRD results. Photoluminescence spectroscopy detected the bacteria attachment to the QDs by showing significant blue shift in bacteria conjugated ZnS QDs. Fluorescence microscopy confirmed the fluorescent labelling of QDs to *Thiobacillus novellus* bacteria cells making them ideal for bio-labelling applications.**

Keywords. **ZnS colloidal QDs; chitosan; sulphate-reducing bacteria; *Thiobacillus novellus*; bio-labelling.**

1. Introduction

Semi-conductor nano-crystals represent a class of quantum confined objects in which the motion of charge carriers are confined to one, two and three dimensions [1]. If the confinement occurs in all the three dimensions, then the zero-dimensional nano-crystal is called quantum dot (QD). Due to quantum confinement effects, QDs act like artificial atoms, showing controllable discrete energy levels [2]. These are characterized by the spacing between the energy levels, which can be tuned by varying the size of the QD. In comparison with the organic dyes and fluorescent proteins, QDs have unique optical and electronic properties like broad absorption spectra, narrow emission bands, high extinction coefficients, good photo stability and reasonably long photo excited lifetimes [3]. These remarkable features enable QDs to have potentially useful technological applications such as photo oxidizers and photo catalysts [4], photovoltaic solar cells [5], optical sensitizers [6], chemical sensors [7], light emitting devices [8], fluorescent probes in biological imaging [9,10] and drug delivery [11].

Zinc sulphide (ZnS) is a semi-conductor luminescent material with a wide band gap energy of 3.61 eV. The band gap can be further increased by doping the ZnS with transition metal ions like Mn^{+2} and Fe^{+3} ions. The initial adsorption of impurities on the nanocrystal surface during growth is known as 'doping' and the compound used is known as 'doping agent'. Doping efficiency is determined by three main factors: surface morphology, nanocrystal shape and surfactants in the growth solution [12,13]. By varying the doping concentrations, the photo-luminescent intensity of the QDs can be manipulated [14]. ZnS is less toxic compound compared to other synthesized QDs (CdSe, PbS) till now. ZnS QDs are hydrophobic in nature, making them insoluble in water. Modification of surface of these QDs by suitable capping agents such as chitosan makes these nanocrystals water soluble and biocompatible.

Chitosan [β-(1 → 4)-2-amino-2-deoxy-d-glucose], which is a natural cationic biopolymer-produced by N-deacetylation of chitin, is a promising alternative capping agent for stabilizing nanosize particles for a wide range of applications. Chitosan molecules contain a large number of chemical functionalities, such as hydroxyl (–OH) and amino ($–NH_2$) groups, resulting in strong adsorption and chelating properties with all types of metal ions. These features have drawn attention to chitosan as a suitable biocompatible

*Author for correspondence (sonal.mazumder@pilani.bits-pilani.ac.in)

and water-soluble polymer for the synthesis of QDs for biological applications [15].

Corrosion is the destructive attack of a material by reaction with its environment and a natural potential hazard associated with oil and gas production and transportation facilities. Microbiologically influenced corrosion (MIC) is the participation of microorganisms in the process nonetheless induces several unique features, the most significant being the modification of the metal–solution interface by biofilm formation [16]. Some sulphate-reducing bacteria produce hydrogen sulphide, which can cause sulphide stress cracking [17]. Hence, it has become important to rapidly detect and identify bacteria.

In this research, chitosan-encapsulated ZnS : M QDs (M = Mn^{2+} or Fe^{3+}) have been synthesized using chemical precipitation method. Parameters like band gap and particle size are estimated by doping the crystal at different molar ratio concentrations ([M]/[Zn^{2+}]) of 0, 2, 4, 6, 8 and applied for fluorescent labelling of sulphate-reducing bacteria, *Thiobacillus novellus*. There is hardly any literature that supports the detection and identification of this corrosive bacteria by QDs. Therefore, it would be worthwhile to explore the possibility of attaching the bio-polymer-capped QDs to the surface of the bacteria.

2. Experimental

2.1 *Materials*

All reagents and precursors purchased were of ultrapure grade. Zinc nitrate hexahydrate ($Zn(NO_3)_2{\cdot}6H_2O$, molecular weight 297.48) was purchased from Sigma Aldrich, Bangalore. Sodium sulphide (Na_2S, molecular weight 78.04 g mol^{-1}) was purchased from Sigma Aldrich, Bangalore. Sodium hydroxide (NaOH, molecular weight 40 g mol^{-1}) was purchased from Merck, Mumbai. Acetic acid (CH_3 COOH, HPLC grade assay: 99.8%, molecular weight 60.01) was purchased from Rankem Limited, Faridabad. Chitosan with low molecular weight and degree of de-acetylation of 80% was purchased from Sigma Aldrich, Bangalore. Ferric nitrate nonahydrate ($Fe(NO_3)_3{\cdot}9H_2O$, molecular weight 404) and manganese acetate ($Mn(CH_3COO)_2$, molecular weight 173.03) was purchased from Sigma Aldrich, USA. N-pentane (C_5H_{12}, assay: 99%, molecular weight 72.15) was purchased from Spectro-Chem Pvt. Ltd., Mumbai. Millipore double distilled water was used for cleaning purposes.

2.2 *Synthesis of chitosan-capped ZnS : M QDs (M = Mn or Fe)*

ZnS QDs were prepared by a chemical precipitation method similar to that reported in the literature [9,18,19]. The main reaction entities were the zinc nitrate hexahydrate, the precipitating agent (sodium sulphide), doping agents (ferric nitrate nonahydrate and manganese acetate) and the capping agent (chitosan).

Chitosan-capped and manganese-doped ZnS QDs [$Zn(1-x)Mn(x)S$] (x = 0, 2, 4, 6, 8 (%)) was synthesized by the following method: 50 ml of chitosan stock solution (0.1% (w/v) in 1% (v/v) aqueous acetic acid solution) was added to the reacting flask.

The pH value of this solution was adjusted to 6.0 ± 0.2 with NaOH (1.0 M). Under magnetic stirring, 50 ml of 0.1 M of $Zn(NO_3)_2{\cdot}6H_2O$ solution and 50 ml of $Mn(CH_3COO)_2$ were added to the reaction flask with mole ratio of [Mn^{2+}] : [Zn^{2+}] = (0, 2, 4, 6, 8, 10) in double distilled water at room temperature and thoroughly mixed. Then the solution was precipitated by adding 50 ml of 0.1 M Na_2S solution drop-wise. Mixture was kept at constant stirring rate at ambient temperature and inert atmosphere. The product mixture was filtered and centrifuged at 10000 rpm for 10 min. The precipitate obtained was washed with double distilled water to remove any excess capping agent and dried in hot air oven at 60°C for 8 h. The procedure was repeated with Fe^{3+} doping using $Fe(NO_3)_3{\cdot}9H_2O$.

2.3 *Sulphate-reducing bacteria*

As explained before, sulphate-reducing bacteria produce hydrogen sulphide, which can cause sulphide stress cracking. Hence, it is imperative to rapidly detect and identify such bacteria. *Thiobacillus novellus* was cultured in nutrition broth medium and bacteria cells are procured.

2.3a *Culturing bacteria*: 100 ml nutrition broth medium was prepared by adding 1.3 g nutrition media to 100 ml double distilled water and autoclaved for 2 h. The solution was cooled down to room temperature and the bacteria strain was added to the nutrition broth medium in laminar hood. The culture medium was incubated at 37°C overnight and bacteria culture successfully procured.

2.3b *Labelling bacteria*: The bacteria was stained on to the glass coverslip by heating at 40°C for 20 min and 0.1 mg of chitosan-capped ZnS QDs were sprinkled onto the glass slide and incubated for 40 min. The glass coverslip was inverted and glycerine added drop-wise before visualizing under fluorescence microscopy.

2.4 *Characterization*

Ultraviolet–visible (UV–Vis) spectra of chitosan-capped ZnS QDs with different doping agents was carried out on absorption mode using Thermo Scientific evolution 201 Spectrophotometer with a wide wavelength range of 200–700 nm. The absorption spectra was used to calculate the band gap energy in the chitosan-capped ZnS QDs and the average particle size of the QDs. All the experiments were conducted in triplicate (n = 3) unless otherwise noted. X-ray diffraction (XRD) pattern of chitosan-capped ZS QDs was recorded on a Rigaku X-ray diffractometer with CuKα radiation operating at 30 kV and 20 mA. Scanning was carried out in 2θ range from 10 to 80° at a scan speed of 2° min^{-1}. The average crystalline size of the ZnS QDs was calculated

using Debye–Scherer formula. Chitosan-capped ZnS QDs are analysed using Fourier transformation infra-red (FTIR) spectroscopy (Perkin Elmer) over a range of 4000–400 cm^{-1}. These samples were prepared by KBr method. It determined the presence of capping agent in the synthesized samples.

Based on the images and selected area, electron diffraction (SAED) patterns, chitosan-capped ZnS QDs were characterized using a Tecnai G2-20-FEI transmission electron microscope (TEM) at an accelerating voltage of 200 kV. Photoluminescence (PL) characterization of QDs were done using LS 55 Perkin Elmer fluorescence spectrometer with excitation $\lambda_{exc} = 265$ nm for analysing the change in the fluorescence spectra with bacterial attachment. Imaging of the fluorescent labelled QDs with *Thiobacillus novellus* bacteria cells was characterized using Olympus BX-41 fluorescence microscopy. A Nikon Coolpix 5.1 mega pixel camera as well as a USB camera with image capture software was used for recording images.

3. Results and discussion

3.1 *UV–Vis spectroscopy analysis*

UV–Vis absorption spectra was used to analyse the formation of chitosan-capped $Zn_xM_{(1-x)}S$ QDs, where (M = Mn^{+2} or Fe^{+3}), ($x = 2, 4, 6, 8$) and to calculate the optical properties of these nano-crystals. The absorption spectra of the chitosan-capped Mn and Fe-doped ZnS QDs are shown in figures 1 and 2, respectively.

The curves represent the absorption bands between 250–400 nm associated with the first excitation transitions in the range of $\lambda_{exc} = 261$–270 nm indicating that the synthesized ZnS QDs are within the 'quantum confinement regime' based on the so called 'blue shift' observed in the curves compared to bulk ZnS ($\lambda_{max} = 343$ nm) [18]. So the optical band gap in chitosan-capped and M-doped ZnS QDs are higher than the bulk ZnS.

The optical band gap and blue-shift values were determined from the absorption coefficient data as a function of wavelength using the 'Tauc relation' as follows:

$$\alpha h\nu = C(h\nu - \Delta E)^n, \tag{1}$$

where C is a constant, α the absorption coefficient, ΔE the average band gap of the material and n depends on the type of transition. For $n = 1/2$, ΔE in equation (1) is direct allowed band gap. The average band gap was estimated from the intercept of linear portion of the $(\alpha h\nu)^2$ *vs.* $h\nu$ plots on x-axis.

The average ZnS nanoparticle size (r) was estimated from an empirical model published in literature [20] using the optical band gap value (ΔE_{QD}) according to equation (2). Therefore, the ZnS : M QDs were produced and stabilized with an estimated average diameter ($2r$) of 3.03 ± 0.2 nm.

$$r(\Delta E_{QD}) = [0.32 - 2.9*(\Delta E_{QD} - 3.49)^{1/2}]/[2*(3.50 - \Delta E_{QD})]. \tag{2}$$

The optical band gap values and the average particle sizes at different doping concentrations of Mn^{+2} and Fe^{+3} are calculated according to the above equations and were tabulated in tables 1 and 2.

If we observe the band gap values at different doping concentrations in tables 1 and 2, then it is clear that initially there is an increase in band gap value with increase in concentration of doping agent and after that it started decreasing. This phenomenon can be clearly emphasized as: in a semi-conductor nano-crystal, when the dopant ions replace the ions of the host lattice, then the crystal lattice is said to be doped and correspondingly band gap value of the crystal increases. As the concentration of the doping ions increases, the dopant ions start absorbing to the surface of the nano-crystal instead of replacing the host ions, resulting an increase in the particle size and change in the surface morphology [13].

Even though, literally, there is less significant change in the band gap values with increase in the doping concentration, it is necessary to optimize it because in nano-regime very small change can affect the properties of the crystals. For example, the application of spherical nano-particles is different from pyramid shape or tube shape particles.

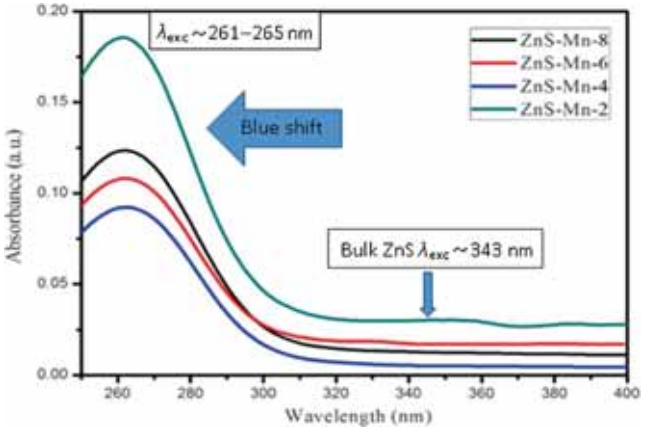

Figure 1. UV–Vis spectra of Mn-doped ZnS QDs.

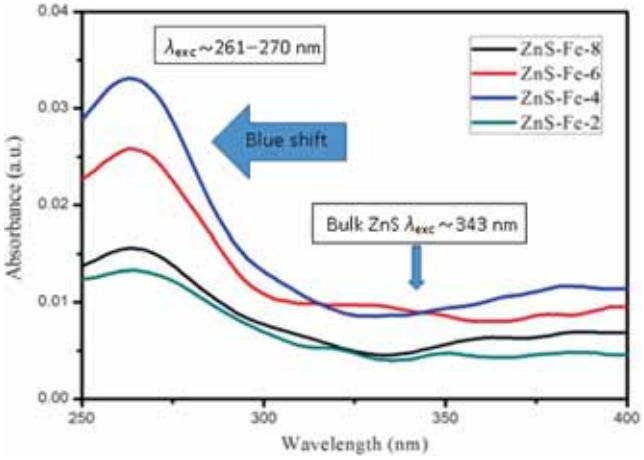

Figure 2. UV–Vis spectra of Fe-doped ZnS QDs.

Table 1. UV–Vis results of Mn-doped chitosan-capped ZnS QDs.

Sample	ΔE_{QD}	Blue shift (eV) Bulk = 3.61	UV–Vis Size 2r (nm)
ZnS-Mn-2	4.248	0.638	2.94
ZnS-Mn-4	4.277	0.667	2.89
ZnS-Mn-6	**4.289**	**0.679**	**2.87**
ZnS-Mn-8	4.268	0.658	2.913

Table 2. UV–Vis results of Fe-doped chitosan-capped ZnS QDs.

Sample	ΔE_{QD}	Blue shift (eV) Bulk = 3.61	UV–Vis Size 2r (nm)
ZnS–Fe-2	4.147	0.537	3.13
ZnS–Fe-4	**4.235**	**0.625**	**2.97**
ZnS–Fe-6	4.189	0.579	3.05
ZnS–Fe-8	4.168	0.558	3.09

From the analysis, ZnS : Mn-6 and ZnS : Fe-4 QD samples showed optimum band gap value and particle size (As shown in bold in tables 1 and 2). The increase in band-gap energy of a semiconductor determines the increase in electrons and holes life-time. Thus, it is expected to increase the photoluminescence intensity of nano-crystals.

3.2 *X-ray diffraction analysis*

The XRD patterns of chitosan-capped ZnS : M-4 QDs (M = Mn, Fe) are shown in figure 3. There is not much difference seen with the doping in the XRD profiles and no secondary phase formations are observed. This can be due to low concentration of doping into the crystal. The three peaks observed in the patterns at 2θ ~29.1°, 48.2° and 56.7° could be assigned to the planes (111), (220) and (311), respectively, of ZnS cubic lattice structure as per JCPDS 05-0566 (zinc blend also referred as sphalerite).

The relative increase of the peak broadening for doped samples has been observed. The peak broadening observed is attributed to the occupancy of doping agents in the lattice sites or interstitial space of cubic close packed ZnS host resulting in shrinkage of crystal lattice and formation of small crystals in nano-regime. Thus, the crystalline particle size reduces with doping. This shrinkage or reducing of lattice dimensions due to introduction of doping agent into the lattice can also cause lattice strain due to lattice mismatch. Using full-width at half maximum (FWHM) values, highest intensity of XRD peak corresponding to (111) planes and using the Debye–Scherer formula, the average nano-crystallite size and lattice strains for the samples were calculated. The particle size and lattice strain is computed and tabulated in table 3. It can be observed that the lattice strains have increased with doping the crystal. It attributes to the presence of doping ions in the host crystal lattice. The XRD results were in good agreement with

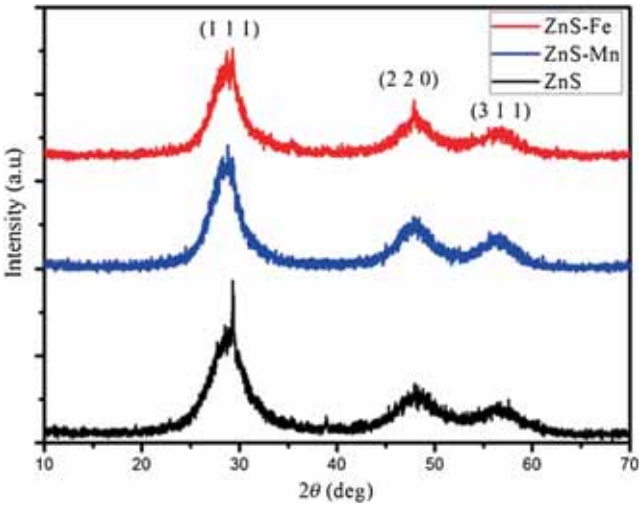

Figure 3. XRD patterns of pure and doped-ZnS QDs.

Table 3. Comparison of XRD results with UV results of ZnS QDs.

Sample	FWHM	Lattice strain	XRD crystalline size (nm)	UV–Vis avg. size 2r (nm)
ZnS	2.451	0.0725	7.42	3.26
ZnS–Fe	3.224	0.3675	2.65	2.97
ZnS–Mn	3.045	0.4236	2.81	2.89

the values obtained for average particle size from UV–Vis absorbance spectra.

3.3 *Fourier transformation infra-red (FTIR) analysis*

FTIR is used to determine the presence of functional groups in the synthesized QDs. In some cases, it has proven to be most important technique in analysing the interaction between the capping agent and the QD [21]. The FTIR spectra of chitosan polymer and chitosan-capped ZnS QD have been shown in figure 4.

In the spectra of chitosan-capped ZnS QDs, the peak at approximately 154 cm^{-1}, which is associated with N–H bending of the primary amine ($–NH_2$), determines the chitosan that is attached to the ZnS QD. All the other peaks like at 2960 cm^{-1} related to strong OH stretching, at 1734 cm^{-1} related to amide group, at 1355cm^{-1} related to C–N stretching of the amine group, which are present in the chitosan polymer are available in the chitosan-capped ZnS QDs, which confirms the encapsulation of chitosan to the ZnS QDs. These amine, amide and hydroxyl groups are the most reactive sites of chitosan which present after conjugation with the ZnS QDs may responsible for further attachment to the biomolecules [22].

3.3a *Chitosan capping mechanism*: By studying the FTIR spectra of normal chitosan and ZnS QDs conjugated chitosan, the strong narrow peak of amino group can be assigned to the formation of coordination complexes between chitosan

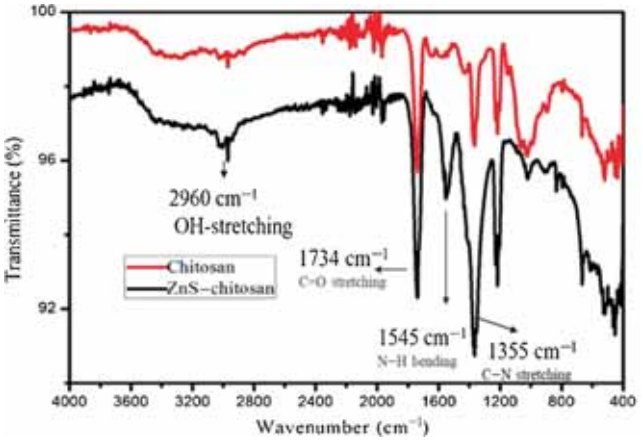

Figure 4. FTIR spectra of chitosan and chitosan-capped ZnS QD.

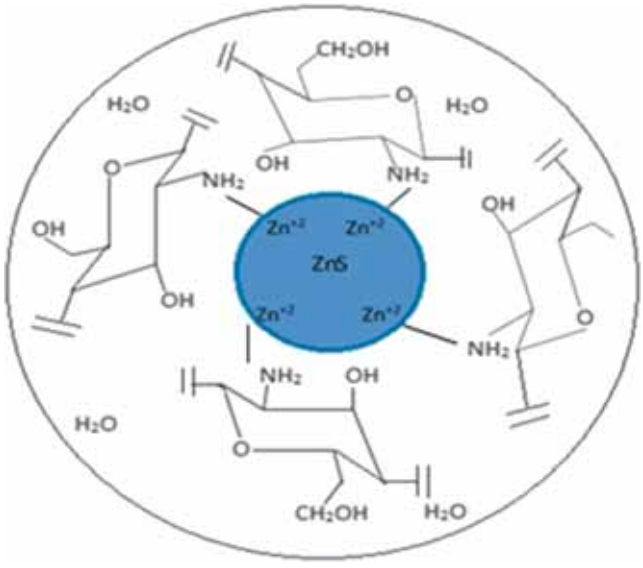

Figure 5. Schematic representation of chitosan-capped ZnS QD.

and zinc cations (Zn^{+2}) on the surface of the QDs. Metal ions have been suggested to be chelated with the NH_2 groups in the chitosan chain as mono and/or multi-dentate ligands (figure 5), depending on the type and concentration of the metal species, the functional derivative groups and the pH level [21].

Chitosan is a pH sensitive polymer and a weak base in aqueous solutions, with a pK_a value of approximately 6.5. This pK_a value leads to the protonation of the amine groups in acid solutions. At lower pH, positively-charged transition metal has to compete with hydrogen ion for complexation with amine electron pair (metal–ligand interactions).

$$\text{Chitosan} - \text{NH}_{2(aq)} + \text{H}^+_{(aq)} \rightarrow \text{Chitosan} - \text{NH}^+_3,$$

$$\text{Chitosan} - \text{NH}^+_{3\,(aq)} + \text{Zn}^{2+}(\text{aq}) \rightarrow [\text{Chitosan} - \text{NH}_2/\text{Zn}^{2+}]_{(aq)} + \text{H}^+_{(aq)}.$$

At higher pH (= 6), the protonation of amine groups is less, thus, more dative bonds can be formed between amine groups and the zinc divalent cations, thus reducing the electrostatic repulsion ($Zn^{2+} \leftrightarrow NH^+_3$) and favouring the stabilization of the ZnS nanocrystals at smaller dimensions due to the increase of the number of nucleation sites [21].

3.4 *Transmission electron microscopy (TEM)*

In this analysis, the particle size and structural features of the chitosan-capped ZnS : Fe-4 QDs were characterized using TEM and SAED analysis. Figure 6 shows representative samples of chitosan-capped ZnS QDs. Figure 6b shows the particles in the spherical morphology confirming the schematic mechanism of chitosan capping to the ZnS QDs as discussed in FTIR analysis. The electron diffraction pattern of the QDs with a lattice parameter comparable to the ZnS cubic crystal (JCPDS 05–0566) is shown in figure 6c. The TEM results confirm that the size of the particles are less than 5 nm with an average particle size of 3.5 ± 0.2 nm. These results are also in good agreement with the average particle sizes given by previous characterizations of UV–Vis and XRD.

3.5 *Photoluminescence (PL) spectroscopy analysis*

By the absorption curves and optical band gap energies evaluated under excitation, ZnS QDs are expected to fluorescence under UV radiation. The PL peaks of chitosan-capped Mn^{2+} and Fe^{3+}-doped ZnS QDs have been fitted using Gaussian fitting tools in ORIGIN software.

3.5a *PL spectra of unconjugated chitosan-capped ZnS : M QDs*: The Photoluminescence of Mn^{2+} doped ZnS QDs highly depends on the lattice position occupied by Mn^{2+} ions in the ZnS host lattice. In figure 7, the photoluminescence spectra of chitosan-capped ZnS : Mn-6 QDs is shown.

The emission spectra revealed the effect of Mn^{2+} ions by quenching of the host emission at 450 nm and appearance of new luminescence at 615 nm using excitation wavelength of 265 nm which can be due to the spin forbidden $^4T_1 \rightarrow {}^6A_1$ transitions with $3d_5$ configuration of Mn^{2+} ion [23]. According to the literature [24], when an impurity or doping ion is incorporated into the host lattice, generally two emissions were observed, one is related to the host and the other is related to the doping agent. While sometimes, the effect of doping agent can suppress or quench the host emission. The quenching effect is the field caused by the crystal form on the orbital of the electron in the atom. As a result, the magnetic moment of the electron is reduced. Hence, as the doping concentration increases there is a considerable decrease in the intensity. In QDs, the doping ion activated on the host would only lead to luminescence when excited with UV radiation but not to their own luminescence property of the doping material. In our case, the Mn^{2+} ions are well incorporated in the host lattice, which is also in agreement with the XRD results. Finally, the blue emission originated from the host

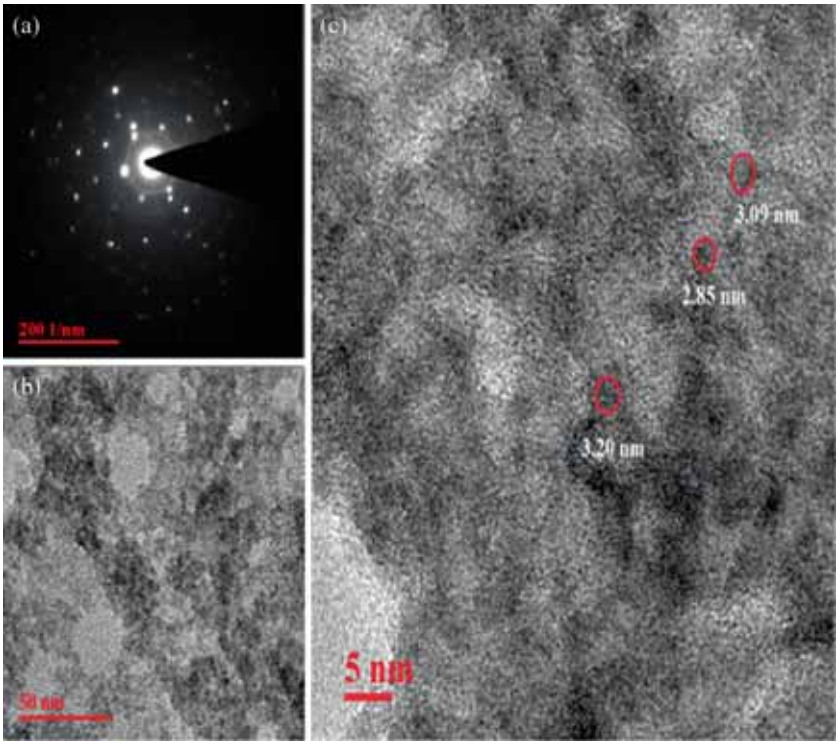

Figure 6. (**a**) SAED pattern of ZnS : Fe-4 QDs confirming crystal planes. (**b**) TEM image of chitosan-capped ZnS : Fe-4 QDs showing the spherical shape particles at 50 nm scale. (**c**) TEM image of chitosan-capped ZnS : Fe-4 QDs at 5 nm scale.

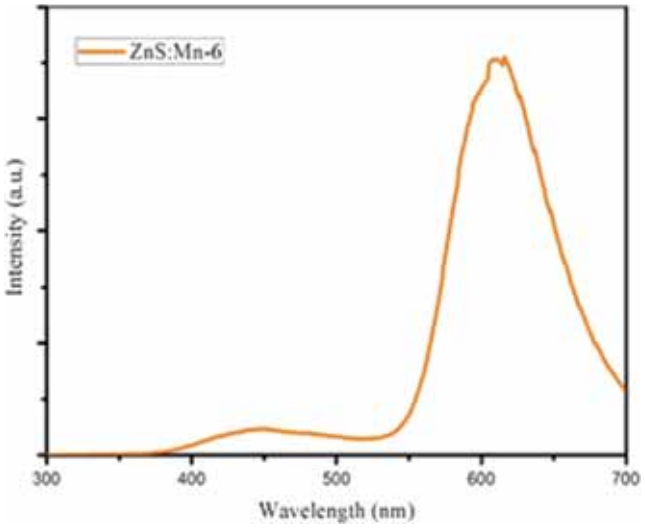

Figure 7. PL spectra of chitosan-capped ZnS : Mn-6 QDs.

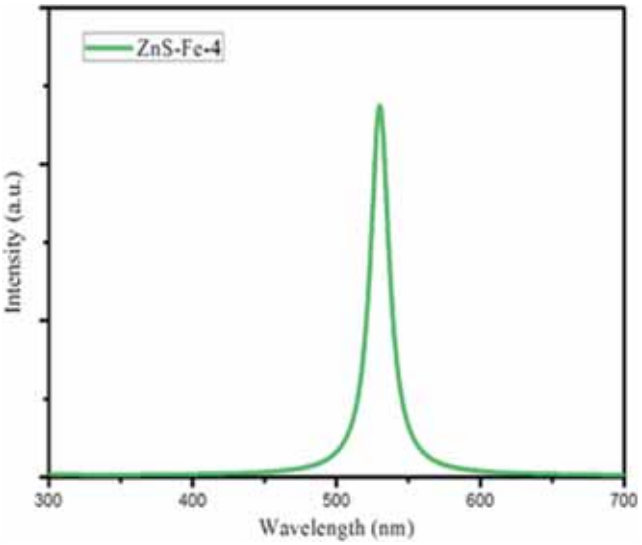

Figure 8. PL spectra of chitosan-capped ZnS : Fe-4 QDs.

ZnS at 450 nm is dominated by the orange emission induced by the Mn^{2+} ion d–d transition.

In figure 8, the photoluminescence spectra of ZnS : Fe-4 QDs is shown. A narrow sharp emission band has been observed around 523 nm, using an excitation wavelength of 265 nm.

In this spectra, the host emission peak has been quenched by the doping agent emission because of the concentration of the Fe^{3+} ions in the host lattice. Such ZnS photoluminescence quenching in the presence of different doping ions has already been reported in the literature [25]. Based on the mechanism proposed in the literature [26], the observed emission signal at 530 nm is due to the transitions from Zn vacancy level to the $^3T_1$ level of exited Fe^{3+} ions in ZnS nanocrystals band gap. Meanwhile, the narrow emission peak can be a sign of high quantum efficiency of this transmission.

3.5b *PL spectra of bacteria conjugated chitosan-capped ZnS : M QDs*: Chitosan-capped ZnS : Mn-6 QDs were used for fluorescent labelling of *Thiobacillus novellus* cells. To confirm the attachment between the QDs and the bacterial cells, photoluminescence spectra was analysed. The attachment is due to the functional groups present in the capping agent and the bacterial cell wall. Initially, the samples were incubated for 1 h at 37°C prior analysis. In figure 9, the photoluminescence spectra of bacteria conjugated ZnS : Mn-6 QDs is shown.

A broad emission band has been observed in the range of 400–700 nm with a peak at around 530 nm, using an excitation wavelength of 265 nm. This shows the blue shift from 615 to 530 nm after the bacteria conjugated with the ZnS : Mn-6 QDs. The obvious shift of these bands suggests that polysaccharides and proteins of the bacterial cells are involved in the attachment of chitosan-capped ZnS : Mn-6 QDs with the *Thiobacillus novellus* cells [27].

In figure 10, the photoluminescence spectra of bacteria conjugated ZnS : Fe-4 QDs is illustrated. The PL spectra results showed a broad emission band in the range of 300–700 nm with two peaks. First peak is at around 490 nm which was generated due to the conjugation of bacteria with the ZnS : Fe-4 QDs. Another narrow peak at around 523 nm can be seen which was the similar peak as in the unconjugated ZnS : Fe-4 QDs as shown in figure 8. This narrow peak may have generated due to the unattached QDs present in the sample. A considerable blue shift from 523 to 490 nm has been observed because of the conjugation of QDs with bacteria cells. The quenching of the fluorescence intensity [28] and broadening of the peak after conjugation has been reported in the literature [29,30] and considered as the confirmation of attachment of the QDs with the bacteria.

These results confirm the bond formation between the chitosan capping agent and the cell membrane of the *Thiobacillus novellus* bacteria. For further analysis on bacterial attachment, fluorescence microscopy has been demonstrated which provide better observation of fluorescent labelling of ZnS QDs to *Thiobacillus novellus* bacteria.

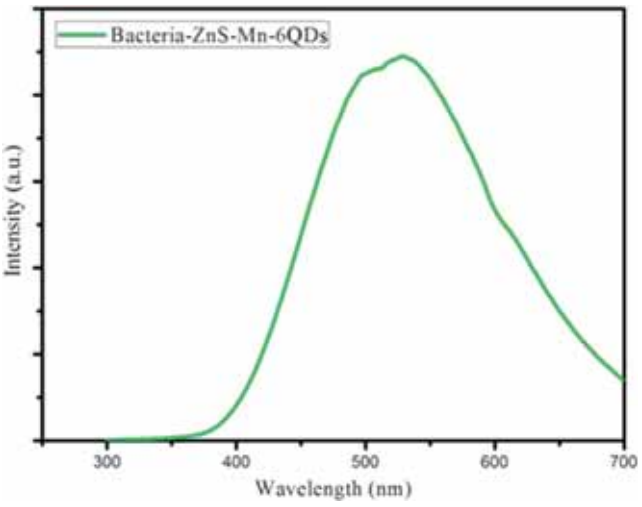

Figure 9. PL spectra of bacteria conjugated chitosan-capped ZnS : Mn-6 QDs.

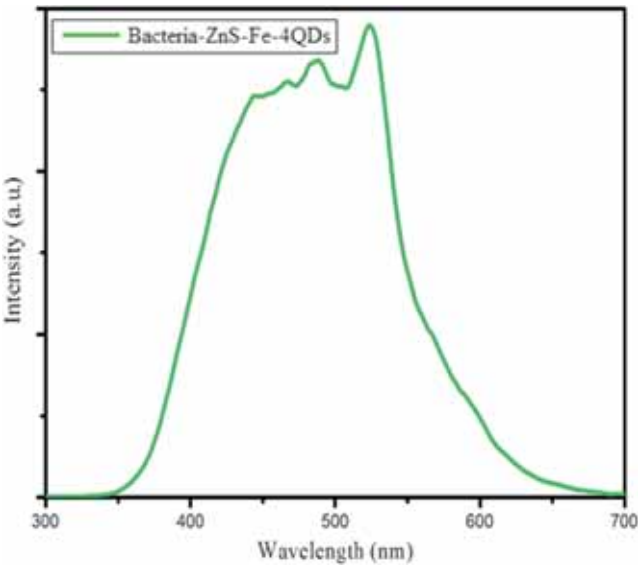

Figure 10. PL spectra of bacteria conjugated chitosan-capped ZnS : Fe-4 QDs.

3.6 *Fluorescence microscopy*

Fluorescence microscopy was able to detect QD-labelled bacterial cells. The images of the *Thiobacillus novellus* bacterial cells incubated with chitosan-capped ZnS QDs for 1 h at 37°C observed under the U filter set (excitation: UG1, 300–400 nm; emission: L420, >420 nm) are shown in figure 11. The Nikon 5.1 mega pixel USB digital camera image of *Thiobacillus novellus* bacteria cells in bright field has been shown in figure 11a and c. It has been observed that the control cells are forming different patterns when kept under incubation. The corresponding fluorescent image in dark field is shown in figure 11b and d.

As seen in the above images, the fluorescing regions match up with the bacterial cell locations. These chitosan-capped ZnS : Mn-6 QDs and ZnS : Fe-4 QDs have a fluorescence maxima at 490 and 523 nm, respectively, as mentioned in the PL analysis. The emission spectra in the form of bacterial cell patterns confirm the attachment of the QDs to the bacterial surfaces. The major part of the area consisting of bacterial cells showing fluorescence, indicating complete coverage of the bacterial cell wall. Even the permeation of QDs through the cell membranes is also a possible criteria because of their very small particle sizes of around 3.5 ± 0.2 nm (<5 nm), which is sufficient for passing through the biological cell membranes [30]. However, for a few cells only the borders are visibly fluorescent, which is indicative of less

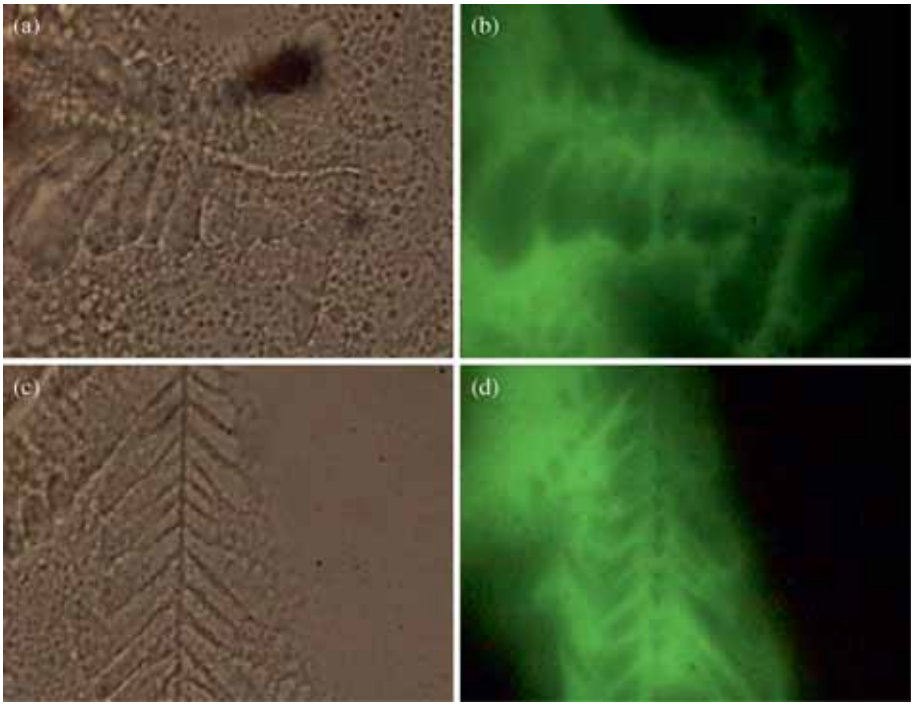

Figure 11. (**a**) Fluorescent microscopy images of the chitosan-capped ZnS : Mn-6 QDs incubated for 1 h with *Thiobacillus novellus* under bright field and (**b**) under U filter set. (**c**) ZnS : Fe-4 QDs incubated for 1 h with *Thiobacillus novellus* under bright field and (**d**) under U filter set.

QD coverage. For these cells, fluorescence is observed from only the outer most edges of the cell wall.

These results clearly show that chitosan-capped ZnS : M QDs (M = Mn^{2+} or Fe^{3+}) can be used for detecting the sulphate-reducing corrosive bacteria.

4. Conclusion

Chitosan-capped ZnS : M QDs (M = Mn^{+2} or Fe^{+3}) were synthesized using a chemical method. UV–Vis spectroscopy results show that the particles were in 'quantum confinement' because of the blue shift and the average particle size was around 3.03 ± 0.2 nm. X-ray diffraction patterns were in the zinc-blend structure (JCPDS 05–0566) and the average crystalline particle size was 2.59 ± 0.3 nm. FTIR confirmed the presence of chitosan in the synthesized QDs. TEM results were in good agreement with the XRD and UV–Vis results with an average particle size of 3.5 ± 0.2 nm. Photoluminescence spectroscopy confirmed the attachment of bacteria to QDs by showing a broad peak. Fluorescence microscopy images concluded the attachment of QDs to the cell walls of *Thiobacillus novellus* bacteria. All these results conclude that chitosan-capped ZnS : M QDs can be efficient fluorescent probes for labelling bacteria.

Synthesizing uniform size QDs in large scale is still a challenge for the researchers. Various parameters like incubation time, dosage and surface charge of the QDs have significant effect on the attachment of bacteria where the future research has to be focussed.

Acknowledgements

We acknowledge the Department of Chemical Engineering, Department of Physics, Department of Biology and Department of Pharmacy at BITS Pilani, Rajasthan, Department of Metallurgical and Materials Science, School of Material Science and Nanotechnology at Jadavpur University, Kolkata, and Materials Research centre, MNIT, Jaipur, for availing their research facility.

References

[1] Schmid Gunter 2004 *Nanoparticles—from theory to application* (Weinheim: Wiley)
[2] Jaszowiec K B 2001 *Acta Phys. Polonica A* **100** 275
[3] Azpiroz J M, Lopez X, Ugalde J M and Infante I 2012 *J. Phys. Chem. C* **116** 2740
[4] Paul A 2000 *Pure Appl. Chem.* **72** 3
[5] Pan Z, Mora-Seró I, Shen Q, Zhang H, Li Y, Zhao K, Wang J, Zhong X and Bisquert J 2014 *J. Am. Chem. Soc.* **136** 9203
[6] Willner Freeman R and Itamar 2012 *Chem. Soc. Rev.* **41** 4067
[7] Chaniotakis Frasco M F and Nikos 2009 *Sensors* **9** 7266
[8] Sun K, Vasudev M, Jung H-S, Yang J, Kar A, Li Y *et al* 2009 *Microelectron. J.* **40** 644
[9] Mazumder S, Sarkar J, Dey R, Mitra M K, Mukherjee S and Das G C 2010 *J. Exp. Nanosci.* **5** 438
[10] Paul A 2004 *Nat. Biotechnol.* **22** 47
[11] Xu Z, Li B, Tang W, Chen T, Zhang H and Wang Q 2011 *Colloid. Surf. B: Biointerfaces* **88** 51

[12] Erwin S C, Zu L, Haftel M I, Efros A L, Kennedy T A and Norris D J 2005 *Nat. Lett.* **436** 91

[13] Dixit N, Anasane N, Chavda M, Bodas D and Soni H P 2012 *Cryst. Res. Technol.* **47** 1105

[14] Hu H and Zhang W 2006 *Opt. Mater.* **28** 536

[15] Mazumder S, Dey R, Mitra M K, Mukherjee S and Das G C 2009 *J. Nanomater.* **2009** 815734

[16] ChineduI O 2012 *Int. Scholar. Res. Network* **570143** 10

[17] Dinh H T, Kuever J, Mußmann M, Hassel A W, Stratmann M and Widdel F 2004 *Nature* **427** 829

[18] Ramanery F P, Mansur A A P and Mansur H S 2013 *Nanoscale Res. Lett.* **512** 8

[19] Rajabi H R, Khani O, Shamsipur M and Vatanpour V 2013 *J. Hazard. Mater.* **250** 370

[20] Mansur H S, Mansur A A P, Araújo A S and Lobato Z I P 2015 *Green Chem.* **17** 1820

[21] Ramanery F P, Mansur A A P, Borsagli F G L M and Mansur H S 2014 *J. Nanopart. Res.* **2504** 1

[22] Tan W B, Huang N and Zhang Y 2007 *J. Colloid Interf. Sci.* **310** 464

[23] Masanori T 2002 *J. Lumin.* **100** 163

[24] Joicy S, Saravanan R, Prabhu D, Ponpandiand N and Thangadurai P 2014 *Royal Soc. Chem. Adv.* **4** 44592

[25] Khani O, Rajabi H R, Yousefi M H, Khosravi A A, Jannesari M and Shamsipur M 2011 *Spectrochim. Acta Part A* **79** 361

[26] Slack G A, Ham F S and Chrenko R M 1966 *Phys. Rev.* **152** 376

[27] Bhadraa P, Mitrac M K, Dasa G C, Deya R and Mukherjeeb S 2011 *Mater. Sci. Eng. C* **31** 929

[28] Hahn M A, Tabb J S and Krauss T D 2005 *Anal. Chem.* **77** 4861

[29] Kloepfer J A, Mielke R E, Wong M S, Nealson K H, Stucky G and Nadeau J L 2003 *Appl. Environ. Microbiol.* **69** 4205

[30] Kloepfer J A, Mielke R E and Nadeau J L 2005 *Appl. Environ. Microbiol.* **71** 2548